

Dynamic vibration analysis of cantilever beams on nonlinear fractional viscoelastic foundation under Gaussian white noise

Jingguo Qu¹, Yuhuan Cui¹, Mengyao Cui¹, Yiming Chen², Aimin Yang¹, and Qianqian Fan¹

¹North China University of Science and Technology

²Yanshan University

March 08, 2024

Abstract

This paper presents the dynamic response of cantilever beam on fractional-order nonlinear viscoelastic foundation subjected to Gaussian white noise. The control equations of the cantilever beam on viscoelastic foundation are established using Hamilton's principle. The problem is solved using the shifted Chebyshev polynomial algorithm, and the control equations are transformed into a system of nonlinear algebraic equations. Numerical examples analyse the correction error and the second norm error, confirming the effectiveness and accuracy of the algorithm in solving such problems. Furthermore, the algorithm's robustness was verified by comparing the responses of Gaussian white noise and non-Gaussian white noise cantilever beam on the viscoelastic foundation. The study examined the impact of various loads and parameters on the cantilever beam, as well as the effect of different harmonic loads on its stress. The research results are in line with the existing literature. These studies offer valuable guidance for practical engineering and enhance comprehension of the dynamic response of cantilevers on foundation in complex environments.

ARTICLE TYPE

Dynamic vibration analysis of cantilever beams on nonlinear fractional viscoelastic foundation under Gaussian white noise

Yuhuan Cui¹ | Mengyao Cui¹ | Yiming Chen² | Jingguo Qu¹ | Aimin Yang^{1,3,4} | Qianqian Fan¹

¹College of Science, North China University of Science and Technology, Tangshan 063000, China

²School of Science, Yanshan University, Qinhuangdao 066004, China

³Tangshan Intelligent Industry and Image Processing Technology Innovation Center, North China University of Science and Technology, Tangshan 063000, China

⁴Hebei Engineering Research Center for the Intelligentization of Iron Ore Optimization and Ironmaking Raw Materials Preparation Processes, North China University of Science and Technology, Tangshan 063000, China

Correspondence

Corresponding author Jingguo Qu, College of Science, North China University of Science and Technology, Tangshan 063000, China.
Email: qujingguo@ncst.edu.cn

Abstract

This paper presents the dynamic response of cantilever beam on fractional-order nonlinear viscoelastic foundation subjected to Gaussian white noise. The control equations of the cantilever beam on viscoelastic foundation are established using Hamilton's principle. The problem is solved using the shifted Chebyshev polynomial algorithm, and the control equations are transformed into a system of nonlinear algebraic equations. Numerical examples analyse the correction error and the second norm error, confirming the effectiveness and accuracy of the algorithm in solving such problems. Furthermore, the algorithm's robustness was verified by comparing the responses of Gaussian white noise and non-Gaussian white noise cantilever beam on the viscoelastic foundation. The study examined the impact of various loads and parameters on the cantilever beam, as well as the effect of different harmonic loads on its stress. The research results are in line with the existing literature. These studies offer valuable guidance for practical engineering and enhance comprehension of the dynamic response of cantilevers on foundation in complex environments.

KEY WORDS

Cantilever beams, Nonlinear viscoelastic foundation, Shifted Chebyshev polynomials, Correction error, Second norm error, Gaussian white noise

1 | INTRODUCTION

The mechanical properties and potential applications of structures have always been of great interest in engineering and science.^{1,2,3,4} Cantilever beams are widely used structures that exhibit unique mechanical properties in various fields. Cantilever beams made of viscoelastic materials exhibit time-dependent and non-linear properties after loading. Viscoelastic cantilever beams have a wide range of applications in various engineering and scientific fields.^{5,6,7,8} The study of these beams is crucial for a deeper understanding of the mechanical behaviour of materials and structures. In engineering applications, viscoelastic cantilever beams can be designed and analysed to solve a range of problems related to structural vibration, dynamic response and durability. In their study, Hao et al.⁹ investigated the deflection and stress of polymer cantilever beams (PET and HDPE) under different external loads (uniformly distributed and harmonic). Jumel et al.¹⁰ performed a fracture test of a single cantilever beam (SCB) under static loading conditions, focusing on the fracture behaviour of cantilever beams under static loading.

In modern engineering, structures often face complex environments and loads, and are founded on diverse and complex foundation conditions. The properties of these foundation conditions significantly affect the performance and behaviour of the structures. Qu et al.¹¹ studied the dynamic behaviour of viscoelastic foundation plates. Arani et al.¹² focused on composite sandwich panels on viscoelastic Winkler-Pasternak foundations. Zhang et al.¹³ studied buckling and free vibration. Atanackovic et al.¹⁴ investigated the vibration of elastic rods on viscoelastic foundations with complex order fractional derivatives under constant axial force. Meanwhile, Javadi et al.¹⁵ analysed the nonlinear vibration behaviour of Kelvin-Voigt viscoelastic beams

Abbreviations: ANA, anti-nuclear antibodies; APC, antigen-presenting cells; IRF, interferon regulatory factor.

on nonlinear elastic foundations subjected to primary, superharmonic and subharmonic excitation. The cantilever beam on viscoelastic foundation is a design that takes into account the viscoelastic properties of the foundation soil. This is more in line with practical engineering situations than traditional rigid foundation beams. Researchers have investigated key issues such as dynamic response, stability and nonlinear behaviour of cantilever beams on viscoelastic foundation through experimental matching and theoretical analysis. The research and application of cantilever beams on viscoelastic foundation have received considerable attention due to the development of modern engineering and the increasing requirements for structural safety. However, studies in this area are still limited. For example, Hosseini et al.¹⁶ conducted vibration studies on viscoelastic cantilever beams placed on nonlinear elastic foundations, while Jiang et al.¹⁷ investigated the structural instability of freely clamped rectangular and circular beams placed on Winkler foundations.

Establishing and solving the governing equations for a cantilever beams on a viscoelastic foundation is fundamental to analysing the response of this structure. At present, the study of solving the governing equations for viscoelastic cantilever beams in the time domain is relatively limited and challenging. Such equations often involve non-linear and time-varying properties, and various numerical and analytical methods have been proposed by researchers. However, most of the numerical methods require a more difficult solution process for the equations,^{18,19,20} which in some cases may lead to instability of the computational results or accumulation of numerical errors. For example, Çalmış et al.²¹ used the complementary function method to derive the Timoshenko beam theory in the Laplace domain, and in turn used Durbin's numerical inverse Laplace transform method to convert the solution results to the real space. Zhen et al.²² by means of Fourier transform, residual theorem and convolution theorem, converted the Eulerian on a nonlinear basis. The nonlinear partial differential governing equations of Bernoulli beam motion are simplified to two nonlinear Volterra integral equations. In addition, Ouzizi et al.²³ and Javadi et al.¹⁵ applied Galyokin's method to transform the equations related to viscoelastic foundation beams into a coupled fractional order differential system and nonlinear ordinary differential equations. However, the implementation of these methods is relatively complex and challenging. Although feasible, they still present some difficulties when faced with nonlinear, time-varying and multi-scale effects, and do not allow the dynamic response of the governing equations to be solved directly in the time domain. Shifted Chebyshev polynomials are used as a common mathematical tool to obtain the deflection response of cantilever beams on viscoelastic foundation directly in the time domain. Such polynomials play a key role in approximation theory, signal processing, image processing and machine learning due to their special spectral properties and optimal approximation performance.^{24,25,26} In recent years, many researchers have used shifted Chebyshev polynomials to approximate the functions, providing new and effective methods. Nemati et al.²⁷ successfully simplified the equations to a system of linear algebraic equations by using second class shifted Chebyshev polynomials. Tural-Polat et al.²⁸ used third class shifted Chebyshev polynomials (SCP3) to approximate multinomial VO FDEs to achieve an efficient numerical solution. Hosseininia et al.²⁹ successfully solved the time fractional three-dimensional Sobolev equations using two-dimensional shifted Chebyshev basis polynomials of the second class and two-dimensional shifted Chebyshev polynomials of the second class. To solve this problem, we use a shifted Chebyshev polynomial algorithm, which can solve nonlinear fractional order equations efficiently and directly in the time domain. This approach has advantages in dealing with the behaviour of viscoelastic materials. It captures the nonlinear and fractional order properties of the materials more accurately, while maintaining high numerical stability and reducing the accumulation of numerical errors. Wang and Dang et al.^{30,31,32,33} used the shifted Chebyshev polynomials algorithm to solve the control equations of arches, plates and beams of structural mechanics directly in the time domain and to simplify the solution process. Qu et al.³⁴ used shifted Chebyshev wavelets to approximate the deflection function of the governing equations of a viscoelastic axially moving plate and provided the numerical solution of the governing equations. Yang et al.³⁶ used the operator matrix of shifted Chebyshev polynomials to directly approximate the deflection function of the viscoelastic microbeam control equation in the time domain, thereby converting the nonlinear fractional order control equation into the form of an operator matrix. Cao et al.³⁵ used this algorithm to solve the viscoelastic bowing problem under a variable fractional rheology model.

In practical applications, Gaussian white noise is often an unavoidable source of interference. Researchers are dedicated to developing noise control and reduction techniques to minimise the impact of noise on signal quality and system performance. Gaussian white noise is a common source of random interference that is prevalent in practical engineering and natural environments. In the study and application of cantilever beams with viscoelastic foundations, it is essential to understand the effect of Gaussian white noise on deflection. It is important to note that this text already adheres to the desired characteristics and is free from errors. The deflection of cantilever beams is affected by the presence of Gaussian white noise, which induces random oscillations in the system. No changes have been made to the content. The study of this effect is of great theoretical importance and practical value. Therefore, the aim of this study is to analyse the effect of Gaussian white noise on the deflection of cantilever beams with viscoelastic foundation. At present, several scholars have studied Gaussian white noise. Hu et al.³⁷

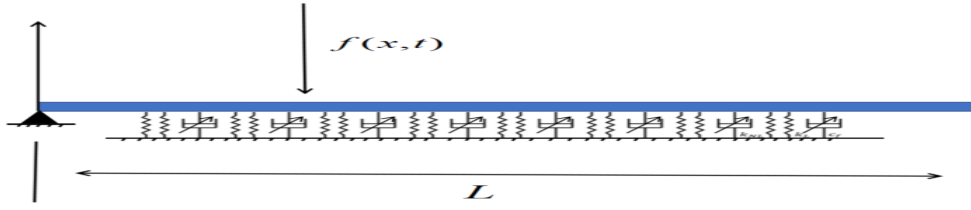


FIGURE 1 Schematic diagram of the cantilever beam on viscoelastic foundation

aim to investigate the stochastic stability of fractional order viscoelastic plates under the influence of Gaussian white noise by determining the p th moment Lyapunov exponent. Malara et al.³⁸ investigate the efficient computation of the nonlinear response of rods containing fractional-order eigenstructure models under stochastic excitation. Loghman et al.³⁹ investigate the vibrational characteristics, stability and response of fractional order viscoelastic microbeams under random excitation. These investigate the vibrational characteristics, stability and response of fractional order viscoelastic microbeams under random excitation. The study, together with others, explored the behaviour of such materials from different perspectives.

The paper is structured as follows: Section II introduces Caputo's fractional order derivatives, which form the theoretical basis. Section III presents the control equations for the cantilever beam on viscoelastic foundation. Section IV introduces the shifted Chebyshev polynomials, an approximation of the deflection function, and a matrix of differential operators for solving the control equations established in section II. Section V examines numerical examples of calculations for cantilever beams. Section VI presents numerical simulations of cantilever beams, taking into account the effect of deflection with different loads, fractional order derivatives, lengths, as well as Gaussian white noise, and analysing the variation of stresses under the action of different simple harmonic loads. Finally, Section VII concludes.

2 | THEORETICAL BASIS

Definition 1. The function $\phi(t)$ is differentiable to order k within $[0, +\infty)$. β definition of Caputo derivative ${}^c D_t^\beta \phi(t)$

$${}^c D_t^\beta \phi(t) = \begin{cases} \frac{1}{\Gamma(k-\beta)} \int_0^t \frac{\phi^{(k)}(\tau)}{(t-\tau)^{\beta+1-k}} d\tau, & 1 \leq k < \beta + 1 < k + 1, k \in N_+ \\ \frac{d^k}{dt^k} \phi(t), & \beta = k \in N_+ \end{cases} \quad (1)$$

where $0 < \beta < 1$, and Γ is the Gamma function, $\Gamma(y) = \int_0^\infty e^{-t} t^{y-1} dt$.

According to the above definition, the derivative of β under the Caputo definition is:

$${}^c D_t^\beta t^k = \begin{cases} 0, & k \in N_0 \text{ and } k < \beta \\ \frac{\Gamma(k+1)}{\Gamma(k+1-\beta)} t^{k-\beta}, & k \in N_0 \text{ and } k \geq \beta \text{ or } k \notin N_0 \text{ and } k > \beta \end{cases}$$

3 | NONLINEAR GOVERNING EQUATIONS OF THE CANTILEVER BEAM ON VISCOELASTIC FOUNDATION

This paper examines a cantilever beam of length L on a nonlinear viscoelastic foundation. As shown in Figure 1, the beam is on a nonlinear fractional viscoelastic foundation and has one end simply supported and one end free. The governing equation is given by Hamilton. Establishing the principle:

$$\delta \int_{T_1}^{T_2} (V - T + W) dT = 0 \quad (2)$$

where T denotes the beam's kinetic energy, V is total strain energy, and W is the amount of work putting in by outside forces.

$$T = \frac{1}{2} \rho A \int_0^L \left(\frac{\partial \omega(x, t)}{\partial t} \right)^2 dx \quad (3)$$

where A is the cross-sectional area of the beam, ρ is the density of the beam, and $\omega(x, t)$ is the deflection of the beam axis.

Overall beam strain energy

$$V = \frac{EA}{8L} \left[\int_0^L \left(\frac{\partial \omega(x, t)}{\partial x} \right)^2 dx \right]^2 + \frac{1}{2} EI \int_0^L \left(\frac{\partial^2 \omega(x, t)}{\partial x^2} \right)^2 dx \quad (4)$$

where E is the Young's modulus and I is the moment of inertia, and the strain on the viscoelastic foundation is given by $\varepsilon(x, t) = EA \int_0^L \left(\frac{\partial \omega(x, t)}{\partial x} \right)^2 dx$.

Overall beam strain energy

$$W = \int_0^L f(x, t) \omega(x, t) dx - \int_0^L \left(\frac{1}{2} k_L \omega^2(x, t) + \frac{1}{2} \eta \frac{\partial \omega(x, t)}{\partial t} \omega(x, t) + \frac{1}{4} k_{NL} \omega^4(x, t) + \frac{1}{2} \mu D_T^\alpha \omega^2(x, t) \right) dx \quad (5)$$

where $f(x, t)$ is used to represent the external load which is the cantilever beam on viscoelastic foundation.

The following is the governing equation of the cantilever beam on viscoelastic foundation when Equations 3 4 5 are entered in formula Equation 2:

$$\rho A \frac{\partial^2 \omega(x, t)}{\partial t^2} + EI \frac{\partial^4 \omega(x, t)}{\partial x^4} - \frac{EA}{2L} \frac{\partial^2 \omega(x, t)}{\partial x^2} \int_0^L \left(\frac{\partial \omega(x, t)}{\partial x} \right)^2 dx + k_L \omega(x, t) + \eta \frac{\partial \omega(x, t)}{\partial t} + k_{NL} \omega^3(x, t) + \mu^c D_t^\alpha \omega(x, t) + f(x, t) = 0 \quad (6)$$

4 | THE SHIFTED CHEBYSHEV POLYNOMIALS

In this part, we convert the nonlinear fractional-order integral-differential control equations into algebraic equations using the shifted Chebyshev polynomials to approximate an unknown function. In other words, we simplify the solution of the control problem by discretising the derivative components in the differential equation and turning it into a system of equations.

The following recursive connection is satisfied by first order Chebyshev polynomials in the range $[-1, 1]$:

$$T_{i+1}(x) = 2xT_i(x) - T_{i-1}(x), \quad i \in N_+ \quad (7)$$

where T is a Chebyshev polynomial and $T_0(x) = 1, T_1(x) = x$.

The shifted Chebyshev polynomial of each interval can be discovered by mapping. By including a variable $x = \frac{2t}{L} - 1$ in equation 7, the recursive relation of the shifted Chebyshev polynomial in the range $[0, L]$ is created

$$T_{i+1}(t) = 2 \left(\frac{2t}{L} - 1 \right) T_i(t) - T_{i-1}(t), \quad i \in N_+ \quad (8)$$

where $T_0(t) = 1, T_1(t) = \frac{2t}{L} - 1$.

The general form of the shifted Chebyshev polynomial in the range $[0, L]$:

$$T_i(t) = i \sum_{n=0}^i (-1)^{i-n} \frac{(i+n-1)! 2^{2n}}{(i-n)! (2n)! L^n} t^n, \quad i \in N_+ \quad (9)$$

A matrix that contains the shifted Chebyshev polynomial is as follows:

$$\Phi_n(t) = [T_0(t), T_1(t), \dots, T_n(t)]^T \quad (10)$$

Matrix form

$$\Phi_n(t) = K_t G_n(t) \quad (11)$$

where $G_n(t) = [1, t, t^2, \dots, t^n]^T$. K_t is the coefficient matrix of the shifted Chebyshev polynomial

$$K_t = [k_{ij}]_{i,j=0}^n, k_{ij} = \begin{cases} 1, & i = j = 0 \\ 2 \left(\frac{2}{H} k_{i-1,j-1} - k_{i-1,j} \right) - k_{i-2,j}, & \text{others.} \\ 0, & i < j \end{cases} \quad (12)$$

4.1 | Displacement function approximation

For the infinitely microsquare integrable function $\omega(x)$, the approximate form of the shifted Chebyshev polynomial can be obtained in the localisation domain $[0, L]$.

$$\omega(x) \approx \sum_{i=0}^n a_i T_i(x) = A^T \Phi_n(x) \quad (13)$$

where a_i is the coefficient of the shifted Chebyshev polynomial, $a_i = \frac{1}{k_i} \int_0^L \omega(x) T_i(x) \omega_L(x) dx$, $A = [a_i]_{i=0}^n$. $\Phi_n(x)$ is the shifted Chebyshev polynomial matrix, $\Phi_n(x) = [T_0(x), T_1(x), \dots, T_n(x)]^T$.

The sequence for any continuous two-dimensional function $\omega(x, t) \in L^2([0, L] \times [0, T])$ may be written as

$$\omega(x, t) \approx \sum_{i=0}^n \sum_{j=0}^n w_{ij} T_i(x) T_j(t) = \Phi_n^T(x) W \Phi_n(t) \quad (14)$$

The shifted Chebyshev polynomial has $W = [w_{ij}]_{i,j=0}^{n,n}$ as its coefficient.

$w_{ij} = \frac{1}{k_i k_j} \int_0^L \int_0^T \omega(x, t) T_i(x) T_j(t) \omega_L(x) \omega_T(t) dt dx$. $\Phi_n(x)$ and $\Phi_n(t)$ are the shifted Chebyshev polynomial matrices.

4.2 | Matrix of the shifted Chebyshev polynomials differential operators

4.2.1 | Matrix of the integer differential operator

Definition 2. If a matrix exists H_x^1 satisfying $\Phi_n'(x) = H_x^1 \Phi_n(x)$, H_x^1 is a first-order differential operator matrix of the shifted Chebyshev polynomials. The first derivative

$$\Phi_n'(x) = (K_x G_x(x))' = K_x (G_x(x))' = K_x (K_x^{-1} \Phi_n(x))' = K_x P K_x^{-1} \Phi_n(x) = H_x \Phi_n(x) \quad (15)$$

where $P = [p_{ij}]_{i,j=0}^n$, $p_{ij} = \begin{cases} i, & i = j + 1 \\ 0, & \text{otherwise} \end{cases}$.

Definition 3. If a matrix exists H_x^2 satisfying $\Phi_n''(x) = (K_x P K_x^{-1})^2 \Phi_n(x)$, H_x^2 is known as the second order differential operator matrix of the shifted Chebyshev polynomial. The second derivative $\Phi_n''(x)$ may be written as

$$\Phi_n''(x) = (K_x P K_x^{-1} \Phi_n(x))' = K_x P K_x^{-1} \Phi_n'(x) = (K_x P K_x^{-1})^2 \Phi_n(x) = H_x^2 \Phi_n(x) \quad (16)$$

obviously $H_x^2 = (H_x^1)^2 = (K_x P K_x^{-1})^2$.

The matrix of the integer differential operator of the shifted Chebyshev polynomial is therefore

$$\begin{aligned} \Phi_n^{(m)}(x) &= (K_x P K_x^{-1})^m \Phi_n(x) \\ \Phi_n^{(m)}(t) &= (K_t P K_t^{-1})^m \Phi_n(t) \end{aligned} \quad (17)$$

where K_t is the replacement of t for x in K_x .

Obtain the following formula:

$$\begin{aligned} \frac{\partial^2 \omega(x,t)}{\partial x^2} &\approx \frac{\partial^2 (\Phi_n^T(x) W \Phi_n(t))}{\partial x^2} = \frac{\partial^2 \Phi_n^T(x)}{\partial x^2} W \Phi_n(t) = \Phi_n^T(x) (K_x P (K_x^{-1})^2) W \Phi_n(t) \\ &= \Phi_n^T(x) H_x^2 W \Phi_n(t) \end{aligned} \quad (18)$$

$$\begin{aligned} \frac{\partial^4 \omega(x,t)}{\partial x^4} &\approx \frac{\partial^4 (\Phi_n^T(x) W \Phi_n(t))}{\partial x^4} = \frac{\partial^4 \Phi_n^T(x)}{\partial x^4} W \Phi_n(t) = \Phi_n^T(x) (K_x P (K_x)^{-1})^4 W \Phi_n(t) \\ &= \Phi_n^T(x) H_x^4 W \Phi_n(t) \end{aligned} \quad (19)$$

$$\begin{aligned} \frac{\partial \omega(x,t)}{\partial t} &\approx \frac{\partial (\Phi_n^T(x) W \Phi_n(t))}{\partial t} = \Phi_n^T(x) W \frac{\partial \Phi_n(t)}{\partial t} = \Phi_n^T(x) W (K_t P (K_t)^{-1}) \Phi_n(t) \\ &= \Phi_n^T(x) W H_t^1 \Phi_n(t) \end{aligned} \quad (20)$$

$$\begin{aligned} \frac{\partial \omega^2(x,t)}{\partial t^2} &\approx \frac{\partial^2 (\Phi_n^T(x) W \Phi_n(t))}{\partial t^2} = \Phi_n^T(x) W \frac{\partial^2 \Phi_n(t)}{\partial t^2} = \Phi_n^T(x) W (K_t P (K_t)^{-1})^2 \Phi_n(t) \\ &= \Phi_n^T(x) W H_t^2 \Phi_n(t) \end{aligned} \quad (21)$$

4.2.2 | Matrix of a fractional differential operator

Definition 4. If a matrix exists $H_t^\alpha(t)$, and ${}^C D_t^\alpha \Phi_n(t) = H_t^\alpha(t) \Phi_n(t)$, $H_t^\alpha(t)$ is the shifted Chebyshev polynomial with an fractional differential operator matrix that can be written as:

$$\begin{aligned} {}^C D_t^\alpha \omega(x,t) &\approx {}^C D_t^\alpha (\Phi_n^T(x) W \Phi_n(t)) = \Phi_n^T(x) W {}^C D_t^\alpha \Phi_n(t) \\ &= \Phi_n^T(x) W K_t \left[0 \frac{\Gamma(2)}{\Gamma(2-\alpha)} t^{1-\alpha} \dots \frac{\Gamma(n+1)}{\Gamma(n+1-\alpha)} t^{n-\alpha} \right]^T \\ &= \Phi_n^T(x) W K_t P^\alpha G_n(t) \\ &= \Phi_n^T(x) W K_t P^\alpha K_t^{-1} \Phi_n(t) \end{aligned} \quad (22)$$

Therefore $H_t^\alpha(t) = K_t P^\alpha K_t^{-1}$, where $p^\alpha = \left[p_{ij}^\alpha \right]_{i,j=0}^n$, $p_{ij}^\alpha = \begin{cases} \mathbf{0} & i \neq j \text{ or } i = j = 0 \\ \frac{\Gamma(i+1)}{\Gamma(i+1-\alpha)}, & i = j \neq 0 \end{cases}$.

4.2.3 | Managing nonlinear terms

$$\begin{aligned} &\int_0^L \left(\frac{\partial \omega(x,t)}{\partial x} \right)^2 dx \\ &\approx \int_0^L \left(\frac{\partial \omega(x,t)}{\partial x} \right)^T \left(\frac{\partial \omega(x,t)}{\partial x} \right) dx \\ &= \int_0^L \Phi_n^T(t) W H_x \Phi_n(x) \Phi_n^T(x) H_x W \Phi_n(t) dx \\ &= \Phi_n^T(t) W H_x \int_0^L \Phi_n(x) \Phi_n^T(x) dx H_x W \Phi_n(t) \\ &= \Phi_n^T(t) W H_x A H_x W \Phi_n(t) \end{aligned} \quad (23)$$

where $A = \int_0^L \Phi_n(x) \Phi_n^T(x) dx$.

4.3 | Calculate the governing equations of the cantilever beam on viscoelastic foundation

Insert the above Equations 18 19 20 21 22 23 into Equation 6.

$$\begin{aligned} &\rho A \Phi_n^T(x) W H_t^2 \Phi_n(t) + EI \Phi_n^T(x) H_x^4 W \Phi_n(t) \\ &- \frac{EA}{2L} \Phi_n^T(x) H_x^2 W \Phi_n(t) \Phi_n^T(t) W H_x A H_x W \Phi_n(t) \\ &+ k_L \Phi_n^T(x) W \Phi_n(t) + \eta \Phi_n^T(x) W H_t^1 \Phi_n(t) + k_{NL} (\Phi_n^T(x) W \Phi_n(t))^3 \\ &+ \mu \Phi_n^T(x) W K_T P^\alpha K_T^{-1} \Phi_n(t) + f(x,t) = 0 \end{aligned} \quad (24)$$

Initial and boundary conditions:

$$\omega(0,t) = \frac{\partial \omega(0,t)}{\partial t} = 0 \quad (25)$$

5 | ERROR ANALYSIS AND NUMERICAL EXAMPLES

This chapter starts with an analysis of errors in the proposed algorithm. It then provides a numerical example to calculate the absolute error and correction error, and evaluates the second norm error. The accuracy and stability of the proposed algorithm are thoroughly assessed through error analysis and numerical examples.

5.1 | Error Analysis

This section presents an error analysis of shifted Chebyshev polynomials.

Theorem 1. *Error Analysis.* Assuming that function $\omega(x)$ is an exact solution, $\omega_n(x)$ is the best approximation of the shifted Chebyshev polynomial of $\omega(x)$ on the interval $[0, L]$, $\omega_n(x) = A^T \Phi_n(x)$. Therefore, the error can be expressed as:

$$\|e_n(x)\|_2 = \|\omega(x) - \omega_n(x)\|_2 \leq \frac{H}{(n+1)!} \cdot \frac{L^{n+1}}{2^{2n+1}} \cdot \sqrt{L}$$

Proof. Assuming that $\omega_i(x)$ is the interpolation polynomial of $\omega(x)$ through node $x_i, i = 0, 1, \dots, n$, where $x_i, i = 0, 1, \dots, n$ represents the root of the $n+1$ -order shifted Chebyshev polynomial in $[0, L]$, it can be determined that

$$|\omega(x) - \omega_i(x)| = \left| \frac{\omega^{(n+1)}(\xi)}{(n+1)!} \prod_{i=0}^n (x - x_i) \right|, \xi \in [0, L]$$

Therefore, it is possible to compute the error estimation for the zero-point interpolation of the shifted Chebyshev polynomial.

$$|\omega(x) - \omega_i(x)| = \left| \frac{\omega^{(n+1)}(\xi)}{(n+1)!} \prod_{i=0}^n (x - x_i) \right| \leq \frac{H}{(n+1)!} \cdot \frac{L^{n+1}}{2^{2n+1}}$$

The second norm error between the exact solution $\omega(x)$ and the numerical solution $\omega_n(x)$ can be expressed.

$$\begin{aligned} \|e_n(x)\|_2^2 &= \|\omega(x) - \omega_n(x)\|_2^2 \leq \|\omega(x) - \omega_i(x)\|_2^2 \\ &= \int_0^L |\omega(x) - \omega_i(x)|^2 dx \leq \int_0^L \left(\frac{H}{(n+1)!} \cdot \frac{L^{n+1}}{2^{2n+1}} \right)^2 dx \\ &= \left(\frac{H}{(n+1)!} \cdot \frac{L^{n+1}}{2^{2n+1}} \right)^2 L \end{aligned}$$

among $H = \max_{0 \leq x \leq L} |\omega^{(n+1)}(x)| = \max_{0 \leq x \leq L} |\omega_n^{(n+1)}(x)|$.

By taking the square root of both sides of the equation at the same time, Theorem 1 is proved. \square

Theorem 2. *Convergence Analysis.* The method described in this article uniformly converges on $[0, L]$, meaning that it does so when $n \rightarrow \infty$ and $\|e_n\| \rightarrow 0$.

Proof. Based on the error estimate provided by Theorem 1, it can be concluded that

$$\|e_n(x)\|_2 = \|\omega(x) - \omega_n(x)\|_2 \leq \frac{H}{(n+1)!} \cdot \frac{L^{n+1}}{2^{2n+1}} \cdot \sqrt{L}$$

among $H = \max_{0 \leq x \leq L} |\omega^{(n+1)}(x)| = \max_{0 \leq x \leq L} |\omega_n^{(n+1)}(x)|$.

When $n \rightarrow \infty$, $\|e_n(x)\|_2 = \|\omega(x) - \omega_n(x)\|_2 \rightarrow 0$

Thus, this paper's method uniformly converges within the interval, and Theorem 2 is proven. \square

5.2 | NUMERICAL EXAMPLES

Take the following dimensionless equation as an example, where $f(x, t)$ is found by exact solution

$$\begin{aligned}
& 86.51 \frac{\partial^2 \omega_n(x, t)}{\partial t^2} + (1 \times 10^{-15}) \frac{\partial^4 \omega_n(x, t)}{\partial x^4} - (4.1 \times 10^{-15}) \frac{\partial^2 \omega_n(x, t)}{\partial x^2} \int_0^L \left(\frac{\partial \omega_n(x, t)}{\partial x} \right)^2 dx \\
& + 1290 \omega_n(x, t) + (1 \times 10^3) \frac{\partial \omega_n(x, t)}{\partial t} + (1 * 10^3) \omega_n^3(x, t) + (1 \times 10^4)^c D_t^\alpha \omega_n(x, t) - f(x, t) = 0
\end{aligned} \tag{26}$$

The exact solution of the equation is $\omega(x, t) = x^4 t^2$. Among

$$f(x, t) = 43.255x^4 + (2.4 \times 10^{-1x})t^2 - (1.125 \times 10^{-2})x^2 t^6 + 1290x^4 t^2 + (1 \times 10^3)x^{12} t^6 + (1 \times 10^4)x^4 \tag{27}$$

During the solution process, a residual function is obtained. This function represents the difference between the numerical solution and the exact solution. By calculating the residual function, the precision and accuracy of the numerical solution can be evaluated. Furthermore, analyzing the residual function allows for the calculation of the correction error, which can be used to improve the accuracy of the numerical solution.

The following is the correction error equation and residual function solved through numerical examples:

$$\begin{aligned}
& 86.51 \frac{\partial^2 E_n(x, t)}{\partial t^2} + (1 \times 10^{-15}) \frac{\partial^4 E_n(x, t)}{\partial x^4} - (4.1 \times 10^{-15}) \frac{\partial^2 E_n(x, t)}{\partial x^2} \int_0^L \left(\frac{\partial E_n(x, t)}{\partial x} \right)^L dx \\
& + 1290 E_n(x, t) + (1 \times 10^3) \frac{\partial E_n(x, t)}{\partial t} + (1 * 10^3) E_n^3(x, t) + (1 \times 10^4)^c D_t^\alpha E_n(x, t) = -R_n(x, t)
\end{aligned} \tag{28}$$

where $E_n(x, t)$ is correction error solution, $e_n(x, t)$ is absolute error solution, $e_n(x, t) = |\omega(x, t) - \omega_n(x, t)|$, $R_n(x, t)$ is the residual function,

$$\begin{aligned}
R_n(x, t) = & 86.51 \frac{\partial^2 \omega_n(x, t)}{\partial t^2} + (1 \times 10^{-15}) \frac{\partial^4 \omega_n(x, t)}{\partial x^4} - (4.1 \times 10^{-15}) \frac{\partial^2 \omega_n(x, t)}{\partial x^2} \int_0^L \left(\frac{\partial \omega_n(x, t)}{\partial x} \right)^2 dx \\
& + 1290 \omega_n(x, t) + (1 \times 10^3) \frac{\partial \omega_n(x, t)}{\partial t} + (1 * 10^3) \omega_n^3(x, t) + (1 \times 10^4)^c D_t^\alpha \omega_n(x, t) - f(x, t)
\end{aligned} \tag{29}$$

Figure 2 shows the numerical calculation example, Figure 2a is the numerical solution, Figure 2b is the exact solution, Figure 2c is the absolute error and Figure 2d is the correction error. In the given example, according to the algorithm proposed in this article, when the shifted Chebyshev algorithm takes $n = 4$, the numerical solution and the exact solution are highly consistent, and the error can reach 10^{-6} at some points. At the same time, the correction error can reach 10^{-9} at some points. In other words, this shows that the algorithm is efficient and accurate under the given conditions. At the same time, comparing the obtained absolute error and the correction error, it is found that the correction error is more accurate than the absolute error at some points, which further verifies the feasibility and accuracy of the algorithm.

Furthermore, the two-norm error of the numerical solution and the exact solution is given by

$$\|\omega(x, t) - \omega_n(x, t)\|_2 = \sqrt{\sum_{n=1}^{\infty} |\omega(x, t) - \omega_n(x, t)|^2}$$

Figure 3 shows the second norm error at different orders, Figures 3a 3b 3c shows the second norm error for the order $\alpha = 0.2$, $\alpha = 0.3$, $\alpha = 0.4$ respectively. It can be observed that the second norm error can reach 10^{-6} and 10^{-7} at some points. This demonstrates the excellent performance of the fractional order in error metrics. In particular, as the order of the fractional order increases, the second norm error gradually decreases, further highlighting the significant advantages of the fractional order in improving the accuracy of the algorithm. This observation highlights the flexibility of the fractional order as a parameter and the sensitivity to errors, providing the algorithm with more reliable numerical performance in practical applications.

6 | NUMERICAL SIMULATION OF THE CANTILEVER BEAM ON FRACTIONAL VISCOELASTIC FOUNDATION

This chapter presents numerical simulations of cantilever beam on viscoelastic foundation. The parameters used in subsequent studies are listed in Table 1. Using MATLAB programming, the deflection of the cantilever beam under different loads at $t = 0.8s$ was simulated and a detailed analysis was carried out. In addition, the influence of Gaussian white noise and other parameter changes on the deflection of the cantilever beam is considered, and the stress distribution under different simple harmonic loads

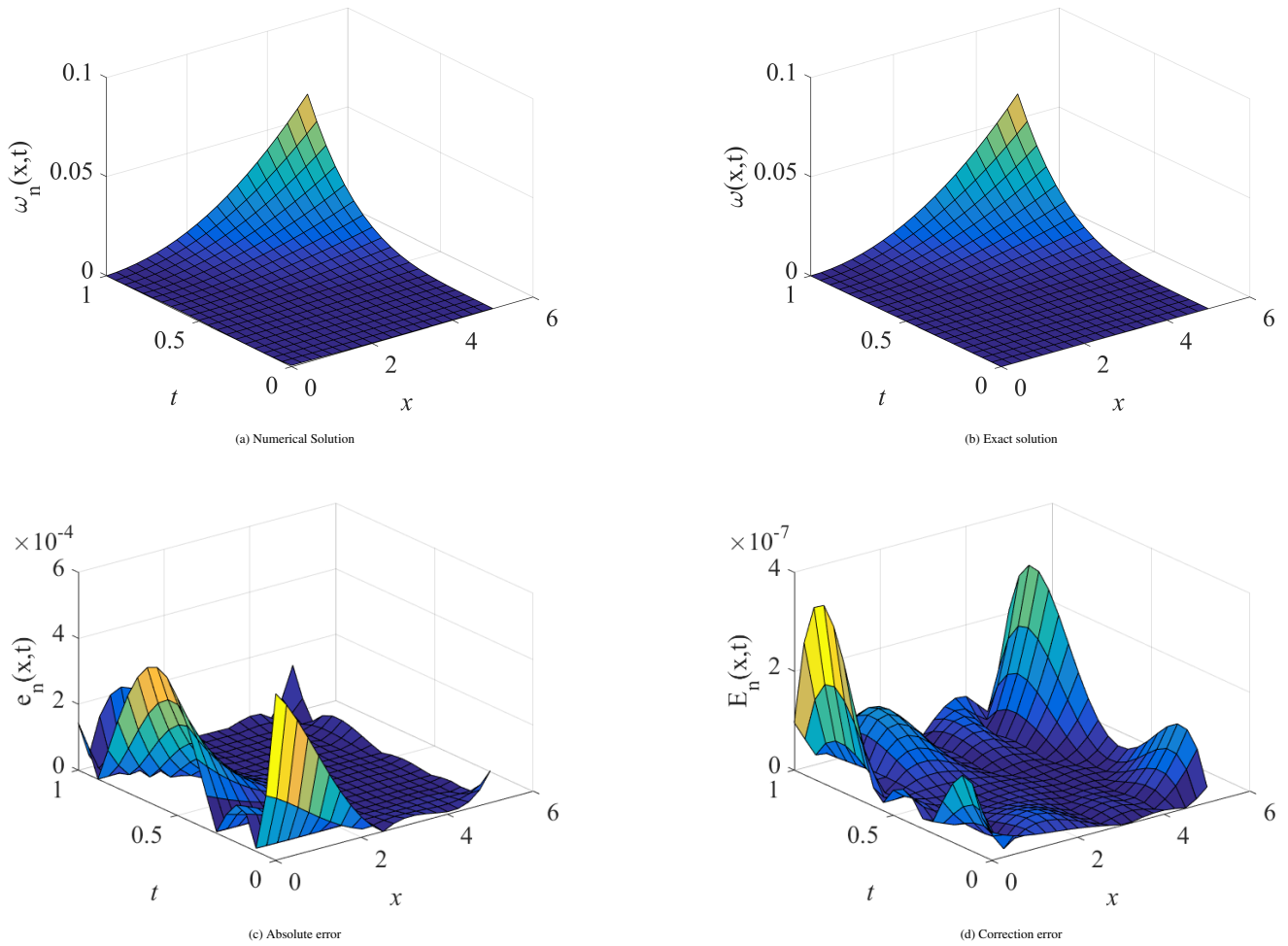


FIGURE 2 Numerical calculation example

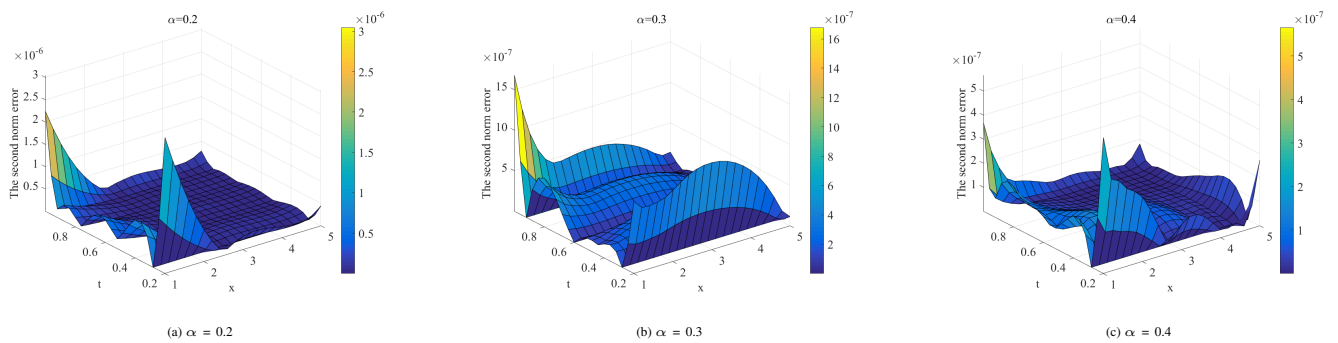


FIGURE 3 The second norm error

is studied in detail. Through these analyses, a deeper understanding of the response and behaviour of cantilever beams in actual engineering can be obtained.

TABLE 1 Parameters of cantilever beams on viscoelastic foundation.

Symbol	Name	Value
A	Cross-sectional area	7.69×10^{-4}
E	Young's modulus	210
I	Second moment of area	1.055×10^5
ρ	Mass density	7850
η	Viscous damping	1.7325×10^6
k_L	Linear stiffness	3.503×10^5
k_{NL}	Nonlinear stiffness	4×10^{14}
μ	Fractional coefficient	1.7325×10^5
L	Length	4

6.1 | Influence of Different Loads on the Deflection of Cantilever Beam on Viscoelastic Foundation

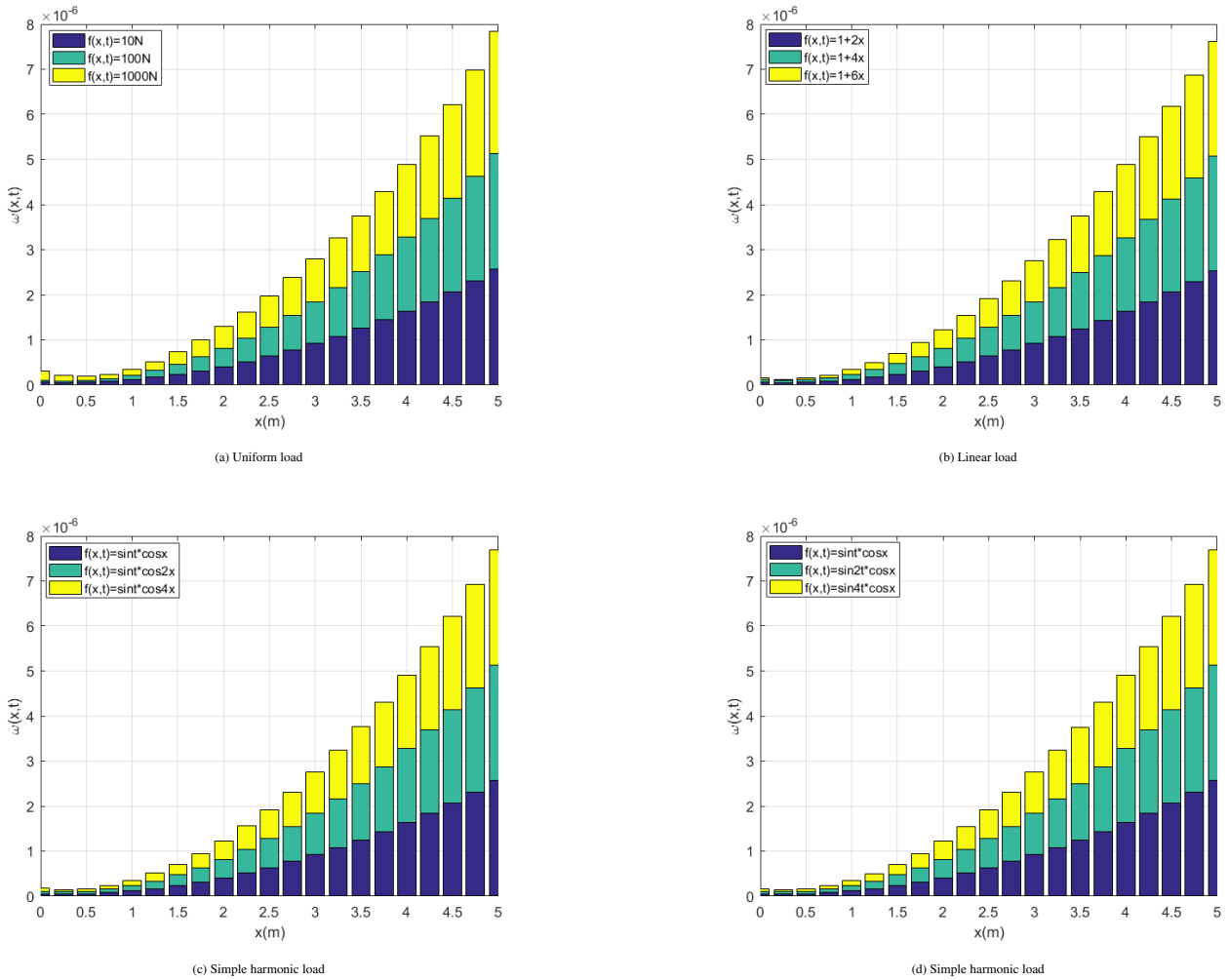


FIGURE 4 Deflection Response of Cantilever Beam on Viscoelastic Foundation Under Different Loads

Figure 4 shows the deflection results of the cantilever beam on the viscoelastic foundation under different loads at $t = 0.8s$. As shown in Figure 1, the left end of the cantilever is simply supported and the right end is free. Looking at Figure 4, we can see

that the deflection of the left end of the cantilever is almost zero, which is in accordance with the boundary conditions. At the same time, the deflection of the cantilever beam increases with the increase of x coordinate and reaches the maximum value at the right end, which is consistent with the actual situation and agrees with the results in the literature.¹⁶

Specifically, Figures 4a, 4b, 4c and 4d show the deflection changes under uniform load, linear load and simple harmonic load respectively. Figure 4a shows the deflection response of the cantilever under the load of $f = 10N$, $f = 100N$ and $f = 1000N$. As the uniform load increases, the deflection of the cantilever on the viscoelastic foundation also increases. Linear load (Figure 4b represents the corresponding deflection under the action of $f = 1 + 2x$, $f = 1 + 4x$ and $f = 1 + 6x$) and simple harmonic load (Figure 4c represents deflection response under the action of $f = \sin t \cos x$, $f = \sin t \cos 2x$, $f = \sin t \cos 4x$, Figure 4d shows $f = \sin t \cos x$, $f = \sin 2t \cos x$, $f = \sin 4t \cos x$) all show similar results, which is consistent with the changing trend of cantilever beam deflection in the existing literature.⁹

These results show that the deflection curve of the numerical simulation agrees well with the experimental results, proving that the adopted numerical algorithm based on shifted Chebyshev has high accuracy. This provides a reliable numerical basis for further in-depth study of the dynamic response of cantilever beams.

6.2 | Influence of Gaussian White Noise on the Deflection of Cantilever Beam on Viscoelastic Foundation

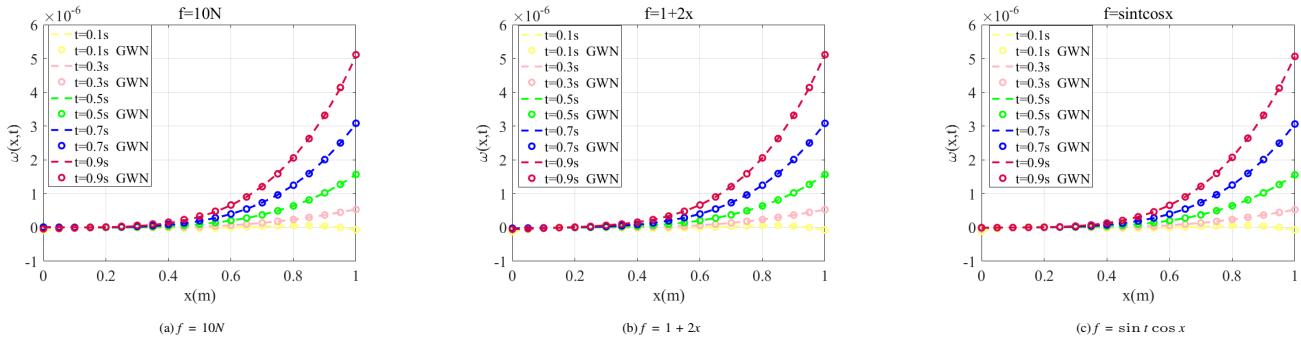


FIGURE 5 Deflection Response of Cantilever Beam on Viscoelastic Foundation Under Gaussian White Noise

Figure 5 displays the cantilever beam on a viscoelastic foundation under different conditions at various times ($t = 0.1s$, $t = 0.3s$, $t = 0.5s$, $t = 0.7s$, $t = 0.9s$). The deflection comparison under load considers the impact of Gaussian white noise and non-Gaussian white noise. The dotted line in the figure represents the deflection change in a non-Gaussian white noise environment, while the circles indicate the deflection in the presence of Gaussian white noise. The acronym 'GWN' is used to represent Gaussian white noise in this context. Different colours are used to represent different time points. Upon observing Figure 5 in its entirety, it becomes apparent that the trend of deflection is consistent with the results presented in the previous section. The deflection of the beam gradually increases over time, which is in line with real-world observations.

Specifically, Figure 5a shows the deflection comparison under the uniform load $f = 10N$. Under the influence of Gaussian white noise, the deflection change is basically the same as without Gaussian white noise, indicating that the shift Chebyshev algorithm is effective in dealing with this type of problem. Figures 5b and 5c show the deflection comparison under the linear load $f = 1 + 2x$ and the simple harmonic load $f = \sin t \cos x$ respectively, which is consistent with the results in Figure 5a. In this section, the algorithm is applied to calculate the deflection response of a cantilever beam on a viscoelastic foundation under the influence of Gaussian white noise. The results show that regardless of the type of load, the shifted Chebyshev algorithm can give the same results as without white noise. Consistent deflection results.

This finding highlights the robustness of the shifted Chebyshev algorithm in dealing with deflection problems of cantilevers on viscoelastic foundations. This algorithm can effectively simulate the deflection response under different types of loads and can maintain basically consistent results even in the presence of Gaussian white noise. Therefore, this algorithm provides a reliable numerical solution method for further research and analysis of the dynamic behaviour of cantilever beams on viscoelastic foundations.

6.3 | Influence of Different Parameters on the Deflection of Cantilever Beam on Viscoelastic Foundation

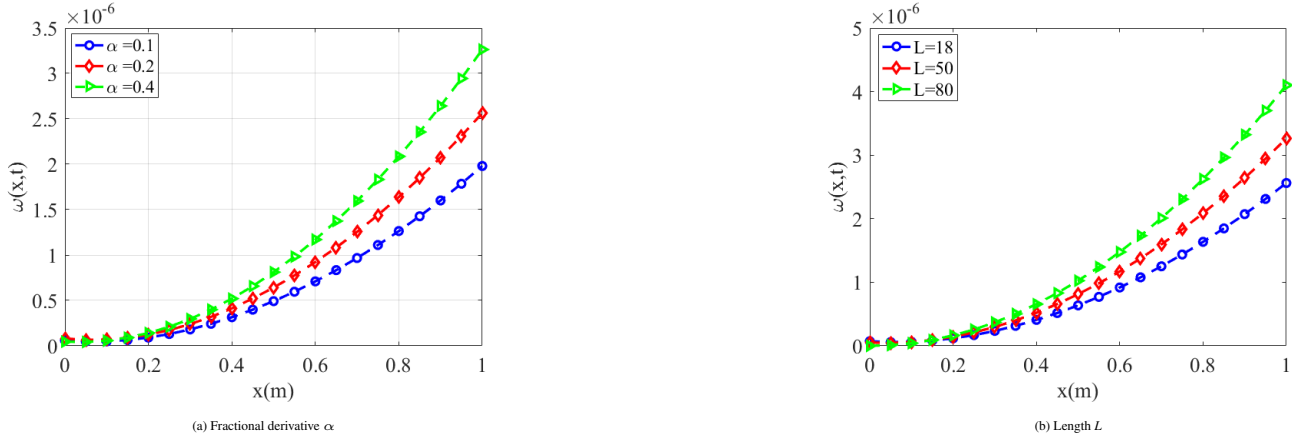


FIGURE 6 Deflection Response of cantilever beam on viscoelastic foundation under different parameters

Figure 6 provides an in-depth study of the influence of different parameters on the deflection of the cantilever on a viscoelastic foundation at $t = 0.8s$, focusing on the fractional order (Figure 6a) and the cantilever length (Figure 6b). At the same time, the accuracy of the shifted Chebyshev polynomial algorithm is verified by comparison with the actual situation.

First, Figure 6a examines the effect of fractional order changes on the deflection of the cantilever beam. The results show that as the fractional derivative increases, so does the deflection of the cantilever. This is because the fractional order can describe the viscoelastic properties of the material and a higher fractional order corresponds to a stronger viscoelastic effect. Therefore, as the fractional order increases, so does the deflection. This result is consistent with the actual situation and confirms the accuracy of the Chebyshev polynomial algorithm in describing viscoelastic behaviour.

Secondly, Figure 6b examines the effect of increasing the length of the cantilever on the deflection. The research results show that as the length of the cantilever increases, so does the deflection. This result is consistent with the results in the existing literature,⁴⁰ further verified the accuracy of the Chebyshev polynomial algorithm when considering the length of the cantilever beam.

Through these systematic studies, a deeper understanding of the influence of different parameters on the deflection of the cantilever beam can be obtained, while the reliability of the adopted algorithm is confirmed.

6.4 | Stress Variation of Cantilever Beam on Viscoelastic Foundation

The stress-strain equation in this section is as follows

$$\sigma(x, t) = E\varepsilon(x, t) + \eta \frac{\partial^\alpha \varepsilon(x, t)}{\partial t^\alpha}$$

Figure 7 shows the change in stress of a cantilever beam on a viscoelastic foundation under different simple harmonic loads. Specifically, Figures 7a 7b 7c represent $f = \sin t \cos x$, $f = \sin t \cos 2x$, $f = \sin t \cos 4x$, respectively. The three-dimensional diagram clearly shows the stress distribution of the cantilever on the viscoelastic foundation and its relationship with time and position under the action of a simple harmonic load.

Specifically, at the fixed end of the cantilever beam ($x = 0m$), the stress of the cantilever beam on viscoelastic foundation reaches the maximum value, which is consistent with the initial conditions of the control equation of the cantilever beam on viscoelastic foundation and is consistent with the results of related literature⁹. Along the x axis, the deformation resistance of the cantilever beam on viscoelastic foundation gradually decreases, so that the stress value of the whole cantilever beam gradually

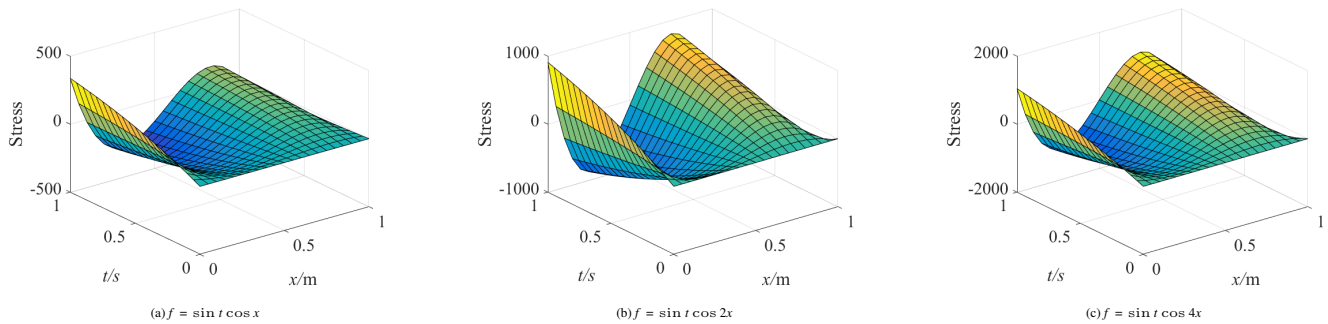


FIGURE 7 Stress Variation of Cantilever Beam on Viscoelastic Foundation

decreases. At the free end of the cantilever ($x = 1m$), the stress of the cantilever on viscoelastic foundation is close to zero, which corresponds to the boundary condition of the cantilever on viscoelastic foundation.

From Figure 7 it can be seen that as the applied simple harmonic load increases, the stress of the cantilever on the viscoelastic foundation also increases. This is because the increase in load causes a greater bending deformation of the cantilever, resulting in a greater stress on the internal materials. Therefore, as the applied load increases, the stress of the cantilever on the viscoelastic foundation will also increase accordingly, which is consistent with the actual situation.

In summary, these observation results show that the stress distribution of the cantilever beam on viscoelastic foundation under the action of a simple harmonic load is consistent with reality and with the initial and boundary conditions of the control equation of the cantilever beam on viscoelastic foundation.

6.5 | CONCLUSION

In this study, the differential control equation of the cantilever beam on viscoelastic foundation was established by using Hamilton's principle, and the shifted Chebyshev was used to directly solve the nonlinear differential-integral equation in the time domain. Through error analysis and numerical examples, the absolute error, correction error and the second norm error of the numerical solution and the exact solution were calculated, and the convergence and accuracy of the algorithm were verified.

The main conclusions of the study are as follows:

1. Under the action of uniform, linear and simple harmonic loads, the deflection of the cantilever beam on viscoelastic foundation increases with the increase of the external load.
2. Under the influence of Gaussian white noise, the deflection is almost the same as that without noise.
3. The deflection increases with increasing fractional order and length.
4. The maximum value of the stress appears at the fixed end of the beam and increases with the increase of the simple harmonic load.

ACKNOWLEDGMENTS

This work is supported by National Natural Science Foundation of China (52074126), the Natural Science Foundation of Hebei Province (E2022209110) in China and the LE STUDIUM RESEARCH PROFESSORSHIP award of Centre-Val de Loire region in France.

CONFLICT OF INTEREST

The authors have no financial or proprietary interests in any material discussed in this article.

REFERENCES

1. Hau LcC, Fung E. Multi-objective optimization of an active constrained layer damping treatment for shape control of flexible beams. *Smart materials and structures*. 2004;13(4):896.
2. Zhang Z, Nie X, Cao J. Variational inequalities of multilayer viscoelastic systems with interlayer Tresca friction: Existence and uniqueness of solution and convergence of numerical solution. *Mathematical Methods in the Applied Sciences*. 2024.
3. Su ZZ, Guo YP. Exact controllability of the transmission string-beam equations with a single boundary control. *Mathematical Methods in the Applied Sciences*. 2023;46(14):15352–15366.

4. Ramírez-Torres A, Penta R, Grillo A. Effective properties of fractional viscoelastic composites via two-scale asymptotic homogenization. *Mathematical Methods in the Applied Sciences*. 2023;46(16):16500–16520.
5. Zhang Z, Zhang Z, Jin X. Investigation on band gap mechanism and vibration attenuation characteristics of cantilever-beam-type power-exponent prismatic phononic crystal plates. *Applied Acoustics*. 2023;206:109314.
6. Wu Z, Xu Z, Qiao H, Chen Y, Chen L, Chen W. Study on anti-progressive collapse performance of assembled steel frame joints with Z-type cantilever beam splices. *Journal of Constructional Steel Research*. 2022;199:107593.
7. Mara'Beh RA, Al-Dweik AY, Yilbas B, Sunar M. Closed form solution of nonlinear oscillation of a cantilever beam using λ -symmetry linearization criteria. *Heliyon*. 2022;8(11).
8. Xiong X, He L, Bao L. Experimental study on flexural behavior of full-scale retard-bonded prestressed UHPC variable section cantilever beams. *Engineering Structures*. 2023;284:115943.
9. Hao Y, Zhang M, Cui Y, Cheng G, Xie J, Chen Y. Dynamic analysis of variable fractional order cantilever beam based on shifted Legendre polynomials algorithm. *Journal of Computational and Applied Mathematics*. 2023;423:114952.
10. Jumel J, Chauffaille S, Budzik MK, Shanahan ME, Guitard J. Viscoelastic foundation analysis of single cantilevered beam (SCB) test under stationary loading. *European Journal of Mechanics-A/Solids*. 2013;39:170–179.
11. Qu J, Zhang Q, Cui Y, Yang A, Chen Y. Dynamic analysis of viscoelastic foundation plate with fractional Kelvin–Voigt model using shifted Bernstein polynomials. *Mathematical Methods in the Applied Sciences*.
12. Arani HK, Shariyat M. Nonlinear 2D-DQ volume-preservative global–local dynamic analysis of composite sandwich plates with soft hyperelastic cores and viscoelastic Winkler-Pasternak foundations. In: . 55. Elsevier. 2023:727–746.
13. Zhang P, Schiavone P, Qing H. Stress-driven local/nonlocal mixture model for buckling and free vibration of FG sandwich Timoshenko beams resting on a nonlocal elastic foundation. *Composite Structures*. 2022;289:115473.
14. Atanackovic TM, Janev M, Konjik S, Pilipovic S, Zorica D. Vibrations of an elastic rod on a viscoelastic foundation of complex fractional Kelvin–Voigt type. *Meccanica*. 2015;50:1679–1692.
15. Javadi M, Rahmanian M. Nonlinear vibration of fractional Kelvin–Voigt viscoelastic beam on nonlinear elastic foundation. *Communications in Nonlinear Science and Numerical Simulation*. 2021;98:105784.
16. Hosseini SM, Kalhori H, Shoostari A, Mahmoodi SN. Analytical solution for nonlinear forced response of a viscoelastic piezoelectric cantilever beam resting on a nonlinear elastic foundation to an external harmonic excitation. *Composites Part B: Engineering*. 2014;67:464–471.
17. Jiang ZC, Ma WL, Li XF. Stability of cantilever on elastic foundation under a subtangential follower force via shear deformation beam theories. *Thin-Walled Structures*. 2020;154:106853.
18. Colbrook MJ, Ayton LJ. A contour method for time-fractional PDEs and an application to fractional viscoelastic beam equations. *Journal of Computational Physics*. 2022;454:110995.
19. Abouelregal AE, Salem MG. The thermal vibration of small-sized rotating fractional viscoelastic beams positioned on a flexible foundation in the light of the Moore–Gibson–Thompson model. *Journal of Ocean Engineering and Science*. 2022.
20. Loghman E, Bakhtiari-Nejad F, Kamali A, Abbaszadeh M, Amabili M. Nonlinear vibration of fractional viscoelastic micro-beams. *International Journal of Non-Linear Mechanics*. 2021;137:103811.
21. Çalim FF. Dynamic analysis of beams on viscoelastic foundation. *European Journal of Mechanics-A/Solids*. 2009;28(3):469–476.
22. Zhen B, Xu J, Sun J. Analytical solutions for steady state responses of an infinite Euler-Bernoulli beam on a nonlinear viscoelastic foundation subjected to a harmonic moving load. *Journal of Sound and Vibration*. 2020;476:115271.
23. Ouzizi A, Abdoun F, Azrar L. Nonlinear dynamics of beams on nonlinear fractional viscoelastic foundation subjected to moving load with variable speed. *Journal of Sound and Vibration*. 2022;523:116730.
24. Kafash B, Delavarkhalafi A, Karbassi SM. Application of Chebyshev polynomials to derive efficient algorithms for the solution of optimal control problems. *Scientia Iranica*. 2012;19(3):795–805.
25. Wang Y, Nie R, Chi P, et al. A novel fractional structural adaptive grey Chebyshev polynomial Bernoulli model and its application in forecasting renewable energy production of China. *Expert Systems with Applications*. 2022;210:118500.
26. Giesbrecht M, Kaltofen E, Lee Ws. Algorithms for computing sparsest shifts of polynomials in power, Chebyshev, and Pochhammer bases. *Journal of Symbolic Computation*. 2003;36(3-4):401–424.
27. Nemati S, Sedaghat S, Mohammadi I. A fast numerical algorithm based on the second kind Chebyshev polynomials for fractional integro-differential equations with weakly singular kernels. *Journal of Computational and Applied Mathematics*. 2016;308:231–242.
28. Tural-Polat SN, Dincel AT. Numerical solution method for multi-term variable order fractional differential equations by shifted Chebyshev polynomials of the third kind. *Alexandria Engineering Journal*. 2022;61(7):5145–5153.
29. Hosseininia M, Heydari M, Razzaghi M. A hybrid spectral approach based on 2D cardinal and classical second kind Chebyshev polynomials for time fractional 3D Sobolev equation. *Mathematical Methods in the Applied Sciences*. 2023;46(18):18768–18788.
30. Wang L, Chen Y, Cheng G, Barrière T. Numerical analysis of fractional partial differential equations applied to polymeric visco-elastic Euler-Bernoulli beam under quasi-static loads. *Chaos, Solitons & Fractals*. 2020;140:110255.
31. Wang L, Chen YM. Shifted-Chebyshev-polynomial-based numerical algorithm for fractional order polymer visco-elastic rotating beam. *Chaos, Solitons & Fractals*. 2020;132:109585.
32. Dang R, Chen Y. Fractional modelling and numerical simulations of variable-section viscoelastic arches. *Applied Mathematics and Computation*. 2021;409:126376.
33. Dang R, Yang A, Chen Y, Wei Y, Yu C. Vibration analysis of variable fractional viscoelastic plate based on shifted Chebyshev wavelets algorithm. *Computers & Mathematics with Applications*. 2022;119:149–158.
34. Qu J, Zhang Q, Yang A, Chen Y, Zhang Q. Variational fractional-order modeling of viscoelastic axially moving plates and vibration simulation. *Communications in Nonlinear Science and Numerical Simulation*. 2024;130:107707.
35. Cao J, Chen Y, Wang Y, Zhang H. Numerical analysis of nonlinear variable fractional viscoelastic arch based on shifted Legendre polynomials. *Mathematical Methods in the Applied Sciences*. 2021;44(11):8798–8813.
36. Yang A, Zhang Q, Qu J, Cui Y, Chen Y. Solving and Numerical Simulations of Fractional-Order Governing Equation for Micro-Beams. *Fractal and Fractional*. 2023;7(2):204.
37. Hu D, Mao X, Han L. Stochastic stability analysis of a fractional viscoelastic plate excited by Gaussian white noise. *Mechanical Systems and Signal Processing*. 2022;177:109181.

38. Malara G, Pomaro B, Spanos PD. Nonlinear stochastic vibration of a variable cross-section rod with a fractional derivative element. *International Journal of Non-Linear Mechanics*. 2021;135:103770.
39. Loghman E, Bakhtiari-Nejad F, Kamali A, Abbaszadeh M. Nonlinear random vibrations of micro-beams with fractional viscoelastic core. *Probabilistic Engineering Mechanics*. 2022;69:103274.
40. Ding H, Chen LQ, Yang SP. Convergence of Galerkin truncation for dynamic response of finite beams on nonlinear foundations under a moving load. *Journal of Sound and Vibration*. 2012;331(10):2426–2442.